Musculoskeletal Imaging PICTORIAL ESSAY

MR Imaging of anterolateral knee pain

Rafaela M. Smarlamaki[1], Foteini I. Terezaki[1], Eirini D. Savva[1], Apostolos Karantanas[1, 2]

[1] *Department of Radiology, School of Medicine, University of Crete, Greece*
[2] *Department of Medical Imaging, University Hospital, Heraklion, Greece*

SUBMISSION: 2/1/2018 | ACCEPTANCE: 11/3/2018

ABSTRACT

The anterolateral knee represents a complex anatomic area including osseous, fatty, tendinous and ligamentous structures. Disorders afflicting this anatomic area include acute trauma, which usually involves more than one structures, repetitive trauma, degeneration, inflammation and tumours and tumour-like lesions. A detailed understanding of the anatomy, biomechanics and pathology of the anterolateral knee is essential for proper imaging interpretation and treatment management. Magnetic resonance (MR) imaging has been established as the method of choice, showing high accuracy in diagnosing painful knees. The present review aims to explore the role of MR imaging in diagnosing the various disorders located in this anatomic area and to present representative cases derived from a single center.

KEY WORDS

MR imaging/diagnosis; knee joint; anterolateral knee/anatomy; anterolateral knee/pathology

1. Introduction

The anterolateral knee (ALk) represents a complex anatomic area consisting of osseous, tendinous, ligamentous and fatty structures. This includes the patella, quadriceps and patellar tendons, lateral patellofemoral ligament (LPFL), fat pads and the anterior horn and body of the lateral meniscus. Although not thoroughly studied, ALk is biomechanically important regarding stability [1, 2]. A wide spectrum of disorders may be seen in the ALk, including tumours and tumour-like disorders. Trauma usually involves more than one of the above structures. Repetitive trauma is demonstrated with tendinopathy, fat pad oedema, bone marrow oedema (BME) and osteochondral injuries. It has been shown that severe anterolateral instability may result in early osteoarthritis in young athletes [3]. Knowledge of the anatomy and

CORRESPONDING AUTHOR, GUARANTOR

Apostolos Karantanas
Department of Medical Imaging, University Hospital, Voutes 71110, Heraklion, Greece, Email: akarantanas@gmail.com

Table 1. Static and dynamic stabilisers of the anterolateral knee with their corresponding restraint action.

Stabilisers anterolateral knee	*Primary*	*Secondary*	*Stabilising action - restraint*
Anterolateral capsule		+	Rotatory knee laxity Anterior laxity
Anterolateral ligament	+	+	Internal rotation of the tibia at knee flexion angles >35° Anterior tibial translation
Iliotibial band/superficial		+	Internal tibial rotation with knee flexion angles >60°
Iliotibial band/middle and deep		+ +	Internal tibial rotation with knee flexion angles >60°-90° In ACL deficiency: Tibial internal rotation from 30° to 90° of flexion Anterior translation lateral tibial plateau

pathology of this area will help radiologists to arrive to a correct diagnosis. The present pictorial essay aims at showing the role of MR imaging in diagnosing the various disorders located in the ALk, with cases derived from a single center.

2. Anatomy and biomechanics

The functional complex of iliotibial band (ITB), ligaments, lateral meniscus and capsule in the ALk provides rotatory knee stability [1, 4, 5]. The *patella* is the largest sesamoid bone in the body and its ossification centers appear between 3 and 6 years and fuse at puberty. It is triangular in shape with a superior base and inferior apex. The posterior surface is smooth, composed of articular cartilage, and is divided into medial and lateral facets. Anatomic variants include the Wiberg II and III morphology which predispose to sub/dislocation [6]. Patellar instability may result from other variations such as trochlear dysplasia, patella alta and tibial tuberosity-trochlear groove distance greater than 20 mm [7]. The *quadriceps femoris* tendon (QFt) inserts on to the superior pole and the *patellar* tendon (Pt) originates from the inferior pole. The *lateral retinaculum* consists of the superficial, oblique and transverse layers [8]. The LPFL and the lateral patellotibial ligament in the deep transverse layer are the two main lateral retinacular structures that stabilise the patella. The LPFL is a palpable thickening of the joint capsule, connects the patella to the femoral epicondyle and its width ranges from 3 to 10 mm [9]. The ITB is a broad fascial structure originating at the iliac crest and terminating at the Gerdy's tubercle at the anterolateral upper end of tibia. It runs down the lateral thigh and knee and passes over the lateral femoral epicondyle. It acts as a hip stabiliser during hip abduction [10]. Due to multiple attachments, including the proximal and distal Kaplan fibers, representing the deep layers, movements like increased femoral abduction and knee internal rotation lead to increased strain and tension on the ITB. The anterolateral *capsule* is composed by the superficial-fibrous and the deep-synovial lamina [11]. It has attachments to the lateral meniscus forming two ligaments, the meniscofemoral and meniscotibial.

The *anterolateral ligament* (ALL) is a distinct ligamentous structure at the anterolateral aspect of the human knee. It was first described by the French surgeon Segond as a "pearly, resistant, fibrous band" along the anterolateral aspect of the knee. The ligament originates on the prominence of the lateral femoral epicondyle, courses obliquely in the anteroinferior direction and inserts at the proximal tibia between Gerdy's tubercle and the fibular head [12-15]. Along its course, it encases the lateral inferior genicular artery and attaches to the peripheral rim of the lateral meniscus. Routine MR imaging protocols are not capable of depicting the ALL in all individuals [16]. Its primary function is to provide anterolateral stability to the knee joint, preventing the proximal tibia from anterior translation [17]. It is also an important stabiliser of internal rotation at flexion, exceeding 35° [18]. Primary and secondary stabilisers in the anterolateral knee are shown in **Table 1**.

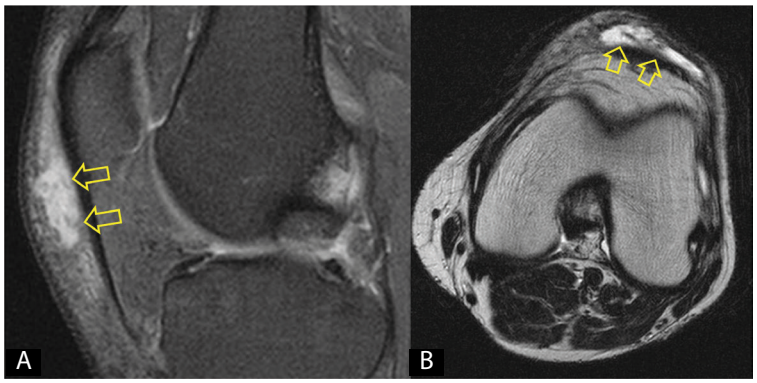

Fig. 1. *A 42-year-old male builder with anterior knee pain and swelling following overuse. Sagittal fat suppressed PD-w (A) and axial T2-w (B) MR images show prepatellar bursitis (open arrows).*

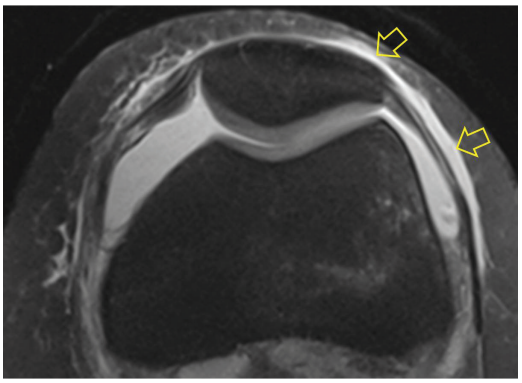

Fig. 2. *Axial fat suppressed PD-w MR image in a 21-year-old-female elite volley ball player, shows a Morel-Lavallee lesion anterolaterally (open arrows) following a bad landing. Joint effusion is also obvious.*

The *infrapatellar fat pad of Hoffa* is one of the three fat pads located in the anterior knee. The others are the *anterior suprapatellar* (SPFP) and the *posterior suprapetellar* (prefemoral-PFFP). Hoffa's fat pad is bounded superiorly by the inferior pole of the patella, inferiorly by the anterior tibia, intermeniscal ligament, meniscal horns and infrapatellar bursa, anteriorly by the patellar tendon and posteriorly by the femoral condyles and the intercondylar notch [19]. Lying intra-articularly but extra-synovially and occupying the whole anterior part of the knee joint, it consists of a central main body with medial and lateral extensions, along with a superior tag, which is not always present. The *anterior horn and body of the lateral meniscus* are located between the corresponding femoral condyle and tibial plateau and are rarely injured. The *osseous structures* involved in ALk pathology include the patella, the anterolateral femoral condyle and the anterolateral tibial condyle.

3. Pathology

3.1 Prepatellar space

The prepatellar bursa is a potential subcutaneous space, present in all individuals. *Prepatellar bursitis* represents fluid accumulation as a result of repetitive trauma, also called *"housemaid's" knee,* acute trauma following a direct fall onto the patella or inflammatory disorders such as rheumatoid arthritis. The most common clinical features are pain, swelling with or without redness and difficulty in kneeling and walking. On MR imaging, prepatellar bursitis appears as a fluid-signal-intensity lesion between the subcutaneous tissue and the patella (**Fig. 1**) [20]. Ultrasound is an alternative method for accurate diagnosis. Treatment is usually conservative. Not all fluid accumulations are symptomatic. Local tenderness clinically and wall enhancement on MR imaging are signs and findings suggesting symptomatic bursitis. A *Morel-Lavallee* lesion is a closed internal degloving injury. The mechanism is usually a blunt shearing force, where the hypodermis is separated from the underlying fascia and the formed cavity is filled with blood and lymph [21]. A fibrous capsule of variable thickness may be formed and may prevent resolution of the effusion. There are two clinical subtypes: the acute and the chronic lesion. Right after or some days after the injury, the lesion is usually large and patients present with a soft-tissue swelling, palpable bulge, bruises and local hypaesthesia [21]. Months after injury, the lesion becomes chronic, is small and firm and clinically may simulate a tumour. A chronic lesion may be complicated with infection. MR imaging is the method of choice for diagnosis, demonstrating signal patterns of haemorrhage depending upon the age of lesion (**Fig. 2**) [21-24]. Treatment depends on the duration, size and capsule thickness of the lesion [25]. Small acute lesions without significant capsule formation require conservative therapy or aspiration. Large and persistent ones with capsule are treated with sclerodesis or surgical debridement and drainage. History and diffuse rather than centrally located effusions favour the diagnosis over the prepatellar bursitis.

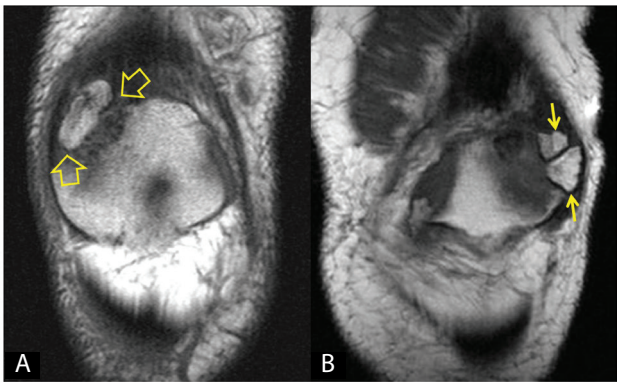

Fig. 3 (left). *Coronal T1-w MR images in two patients, showing bipartite (A) and tripartite (B) morphology of the patella (open arrows).*

Fig. 4. *MR imaging in a 15-year-old male, with anterosuperolateral knee joint pain. Fat suppressed sagittal (A), axial (B) PD-w and coronal STIR (C) images, show the sychondrosis (thin arrows) of the unfused ossification center superolaterally and the bone marrow oedema (open arrows).*

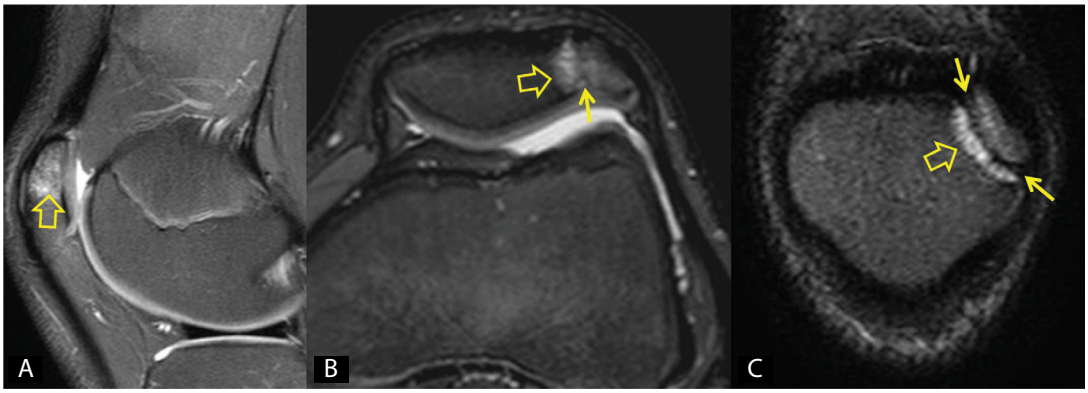

3.2. Patella

In 1-2% of the population, patella develops as two unfused ossification centers connected by thick fibrous tissue, which define the *bipartite* patella, affecting men more than women [26]. This variant is often located supero-laterally and is symptomatic in about 1-2% of cases because of mobility at the synchondrosis [27]. These variants are classified by location (supero-lateral or lateral) and number of fragments (bipartite, tripartite or multipartite). On radiographs, inexperience could lead to mistake the bipartite patella as a patellar fracture. The presence of sclerotic borders on both sides of the interface, as opposed to the sharp fracture line, is diagnostic [26]. Computed tomography (CT) shows clearly the synchondrosis. Coronal T1-w MR images also show this variant (**Fig. 3**). Fluid sensitive sequences are able to match the presence of symptoms with a bipartite patella, by showing BME on both sides of the synchondrosis (**Fig. 4**).

Trauma: Patella may sustain fractures from direct blow, which are best evaluated with plain radiographs. Stress injuries, including stress reactions and fractures, are rare and occur in runners, track athletes and those involved in jumping sports. Patellar stress injuries represent less than 1% of all stress injuries and are high risk if left untreated [28]. They are the result of repetitive microtrauma [29] and are best shown with fluid sensitive MR sequences, sharing the same imaging findings with other stress injuries. The early phase of a stress injury, a stress reaction, shows only BME (**Fig. 5**) and, if not promptly recognised, may proceed to a stress fracture showing a low signal intensity line surrounded by BME. Differential diagnosis of a stress reaction should be made from non-traumatic BME, which is rarely located in the patella in the context of acute bone marrow oedema syndrome (aBMEs) (**Fig. 6**). This is primarily seen in middle aged men with reports showing that underlying osteopaenia or osteoporosis is a common associated and possibly predisposing factor [30]. Acute *avulsion fractures* represent an osteocartilaginous avulsion of the lower pole of the patella in the growing skeleton, before it fully ossifies. It should be suspected in the paediatric knee if symptoms arise after violent loading applied on a flexed knee [31]. The fracture may be difficult to see on a radiograph, especially when the fragment is small or absent (**Fig. 7a**). Radiographs can sometimes demonstrate the disrupted tendon, or more commonly, a patella alta with infrapatellar soft-tissue swelling. Sonography can clearly identify the periosteal avulsion. MR imaging is able to show the extent of the injury, as well as injury of cartilage and ligaments (**Fig. 7b, c**). Avulsions may also oc-

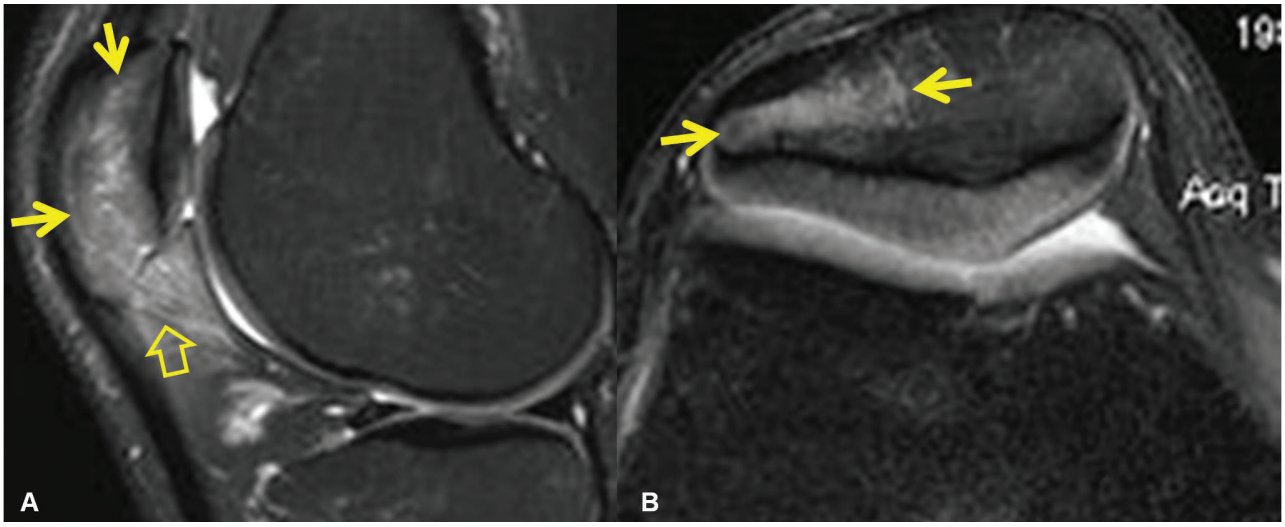

Fig. 5. *MR imaging in a 24-year-old professional young football player (A) and a 12-year-old track athlete (B), without any history of trauma. Fat suppressed sagittal (A) and axial (B) PD-w MR images showing bone marrow oedema in keeping with a stress reaction (arrows). Hoffa's fat pad oedema is also shown (open arrow).*

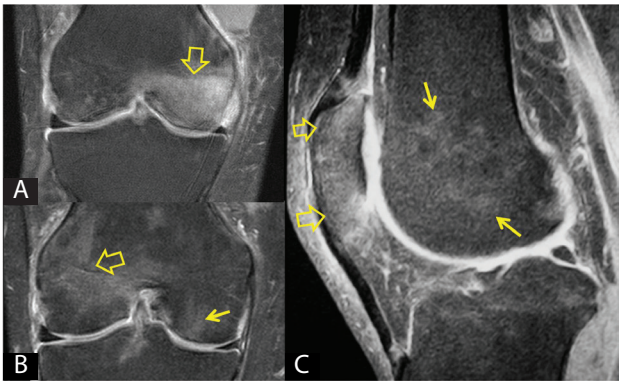

Fig. 6. *A 55-year-old male patient with migrating arthralgia and a spinal DEXA suggesting osteoporosis. A. Coronal fat suppressed PD-w MR image showing BME in the medial femoral condyle (open arrow). B. Three months later, pain was remarkably reduced in keeping with resolution (thin arrow). New pain appeared in the lateral femoral condyle in keeping with imaging findings of BME (open arrow). C. Pain was reduced on imaging follow up 4 months after B. Sagittal fat suppressed PD-w MR image showing resolution of oedema in the lateral femoral condyle (thin arrows) and new BME in the patella (open arrows). The findings are typical of regional migrating osteoporosis (migrating acute bone marrow oedema syndrome).*

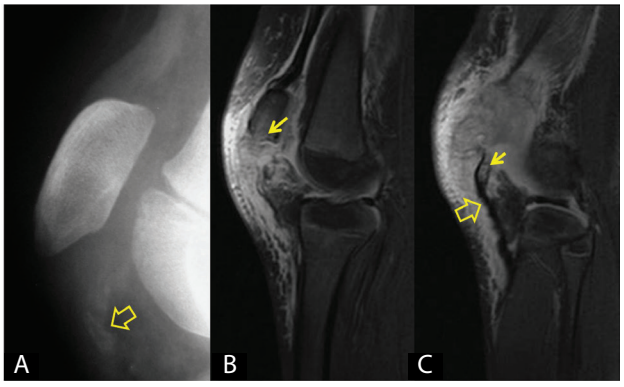

Fig. 7. *A 8-year-old girl presented with anterolateral knee pain and inability to extend her leg after stepping on a ball. A. Lateral view of radiograph hardly shows the avulsed fracture (open arrow). Sagittal fat suppressed PD-w MR images. B. BME and irregular lower pole surface are shown in the patella (arrow). Intra and extraarticular effusion are also shown. C. Lateral to B image, showing the retracted patellar tendon (open arrow) and the avulsed osseous fragment (arrow).*

cur in adolescents, in the distal patellar tendon insertion upon the tibial tubercle. Pathognomonic for recent and reduced lateral patellar dislocation is the presence of BME at the medial patellar facet, with or without associated osteochondral injury, and at the anterolateral femoral condyle (**Fig. 8**) [32]. A careful investigation of associated findings suggesting patella maltracking, such as trochlear dysplasia, abnormal tibial tubercle-trochlear groove distance and patella alta or Wiberg III patellar shape, should be pefrormed [33]. Sulcus angle and depth,

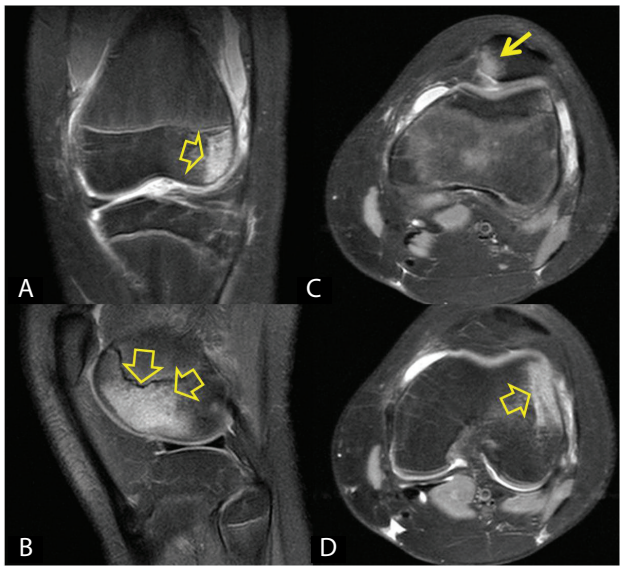

Fig. 8. *A 14-year-old male athlete with a recent rotational injury. Lateral dislocation of the patella, which was reduced spontaneously. Fat suppressed coronal (A), sagittal (B) and axial (C, D) PD-w MR images, showing the typical location of the BME in the lateral femoral condyle (open arrows) and the lower medial patella (arrow).*

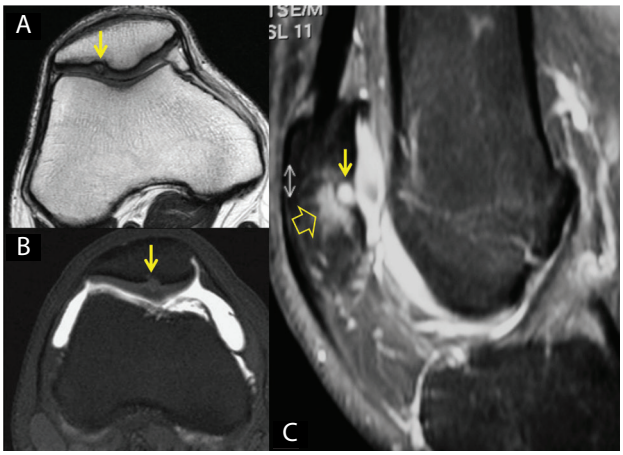

Fig. 9. *Dorsal patellar defect in a 36-year-old male weekend athlete. A. Axial T2-w MR image shows the incidentally found osseous lesion in the lateral patellar facet (arrow). The axial fat suppressed T1-w MR arthrographic image (B) and the sagittal fat suppressed PD-w (C) MR image in a 21-year-old male elite tennis player with anterior knee pain show the defect (arrows) and the surrounding bone marrow oedema (open arrow). A local swelling, in keeping with chondromalacia, is also seen in the overlying articular cartilage, without any fissuring.*

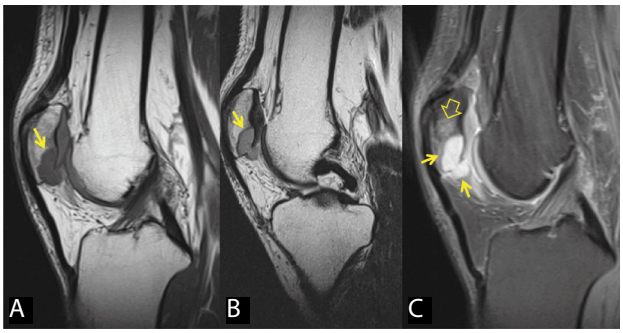

Fig. 10. *A 38-year-old male with a few month anterior knee pain. The sagittal T1-w (A), T2-w (B) and fat suppressed PD-w (C) MR images show an osteolytic lesion in the lower pole of the patella extending to the superior Hoffa's fat pad (arrows) with surrounding bone marrow oedema (open arrow). Histologically the lesion turned out to be a giant cell tumour.*

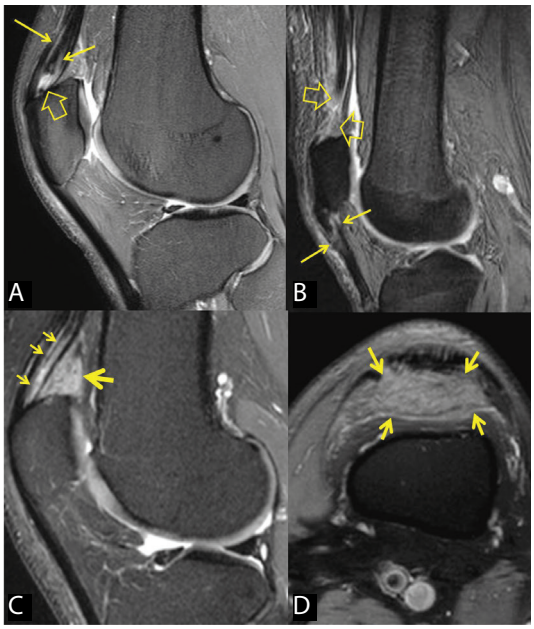

Fig. 11 (right). *A. Elite 36-year-old male volleyball player with anterior suprapatellar pain. Sagittal fat suppressed PD-w MR image showing quadriceps tendinopathy (arrows) and a partial tear (open arrow). B. Sagittal T2* MR image in a 62-year-old male patient with known ankylosing spondylitis and acute-on-chronic anterior knee pain showing a compete tear-discontinuity of the quadricepts tendon insertion (open arrows). Patellar tendinopathy is also shown (thin arrows). Sagittal (C) and axial (D) fat suppressed PD-w MR images in a 34-year-old male who is professionally kneeling and a 60-year-old physician respectively, both with long standing anterior knee pain, show suprapatellar fat pad oedema (arrows). Tendinopathy is shown on C (small arrows)*

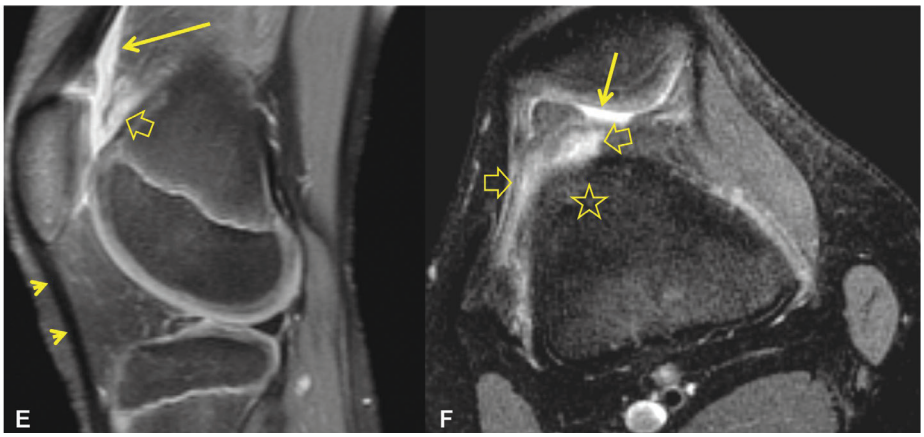

Fig. 11. *Sagittal (E) and axial (F) fat suppressed PD-w MR images in a 9-year-old female synchronised swimmer with anterior knee pain show prefemoral fat pad oedema (open arrows), joint effusion (long arrows), patella alta with elongated patellar tendon (arrowheads) and tochlear dysplasia (*).*

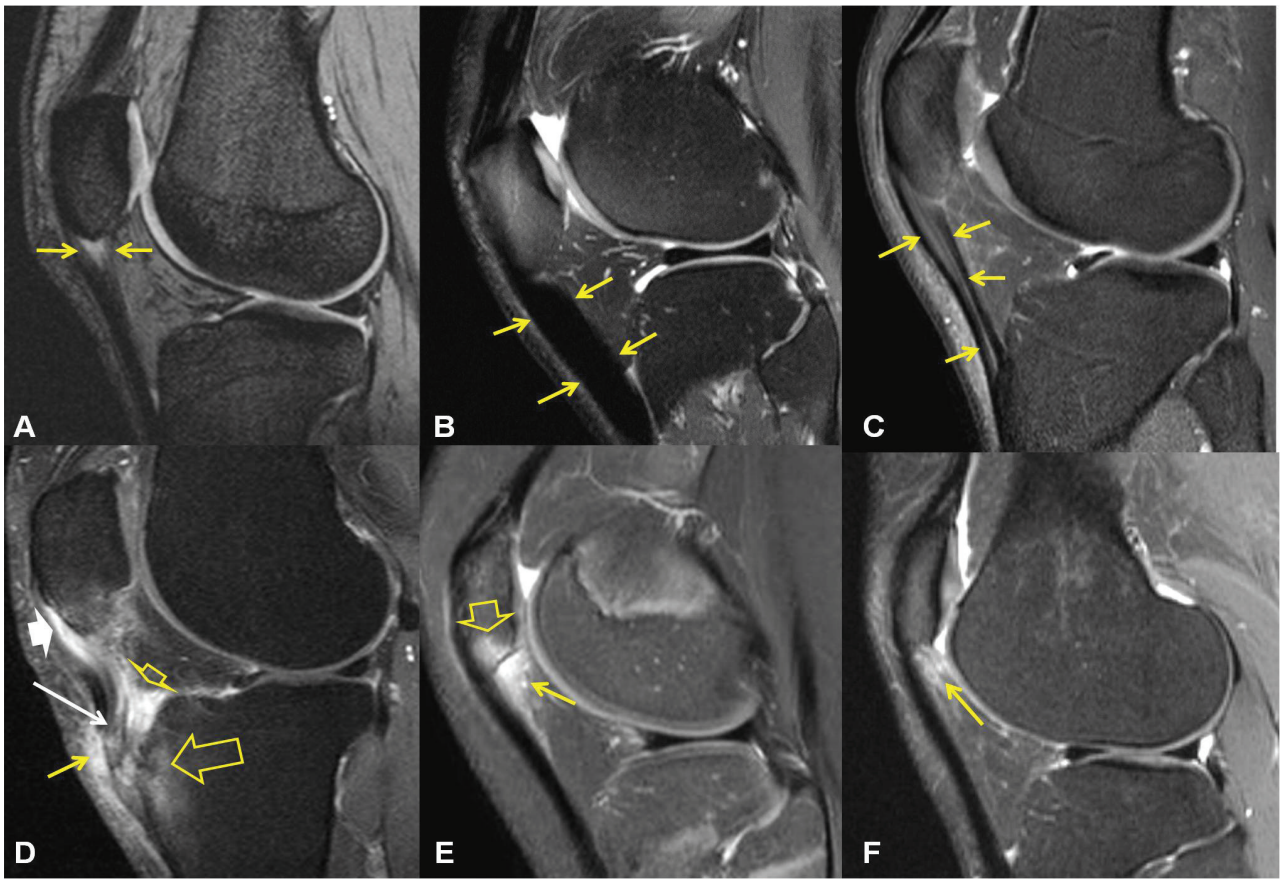

Fig. 12. *A. "Jumper's knee" in 17-year-old football player. Sagittal T2* MR image showing the abnormal signal intensity within the posterior part of the thickened proximal patellar tendon (arrows). Sagittal fat suppressed PD-w MR images showing patellar tendinopathy in a 42-year-old male skier (B) and tendinopathy with mucoid degeneration in a 33-year-old male runner (C) (arrows). D. Unresolved Osgood Schlatter disease 37-year-old previously professional tennis player, with pain during acceleration and deceleration. Sagittal fat suppressed contrast enhanced T1-w MR image showing abnormal enhancement in the proximal (white thick arrow) and distal degenerated tendon (long white arrow), oedema surrounding the patellar tendon insertion (thin arrow) and bone marrow oedema (open arrow). A retropatellar bursitis is also seen (short open arrow). E. Sagittal fat suppressed PD-w MR image in a 13-year-old female athlete showing the findings of early Sinding-Larsen-Johansson's disease with soft tissue infrapatellar oedema (arrow) and bone marrow oedema in the lower pole of the patella (open arrow) without fragmentation. F. Sagittal fat suppressed PD-w MR image in a 30-year-old female with 1-year anterior knee pain showing superolateral infrapatellar fat pad (Hoffa fat pad) oedema in keeping with impingement due to patellar maltracking (arrow).*

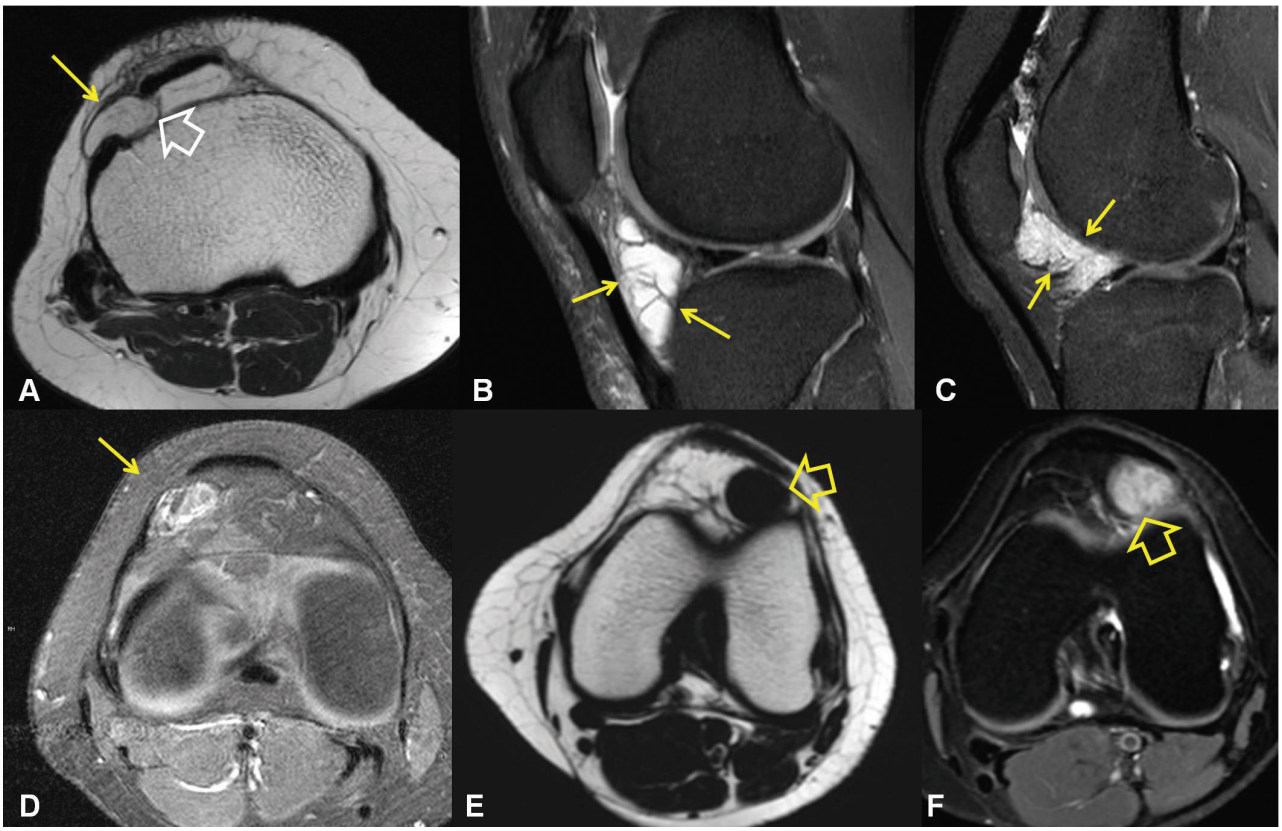

Fig. 13. *Hoffa's fat pad space occupying lesions. A. Axial T1-w MR image in a 50-year-old female patient with anterolateral swelling showing a benign lipoma located in the anterolateral fat pad (white open arrow) and the subcutaneous fat (arrow). B. Sagittal fat suppressed MR image in a 37-year-old male patient with knee joint swelling, showing a ganglion cyst (arrows). C. Sagittal fat suppressed contrast enhanced T1-w MR image in a 17-year-old female patient showing an enhancing synovial haemangioma (arrows). D. Axial fat suppressed contrast enhanced T1-w MR image in a 16-year-old male football athlete with previous steroid injection and anterolateral knee pain showing fat necrosis (arrow). Nodular synovitis in a 30-year-old female showing a mass with low signal on T1-w (E) and high signal on fat suppressed T2-w (F) MR images.*

lateral patellar displacement and lateral patellofemoral angle have shown to correlate with development of *patellofemoral osteoarthritis* [34]. Accelerated osteoarthritis may occur secondary to chondromalacia and chondral injury [35].

Dorsal defect of the patella (DDP) represents an osteolytic lesion on the superolateral aspect of the patella, primarily found in the second and third decades of life. Up to 25-33% of cases, DDP is bilateral. Although the aetiology of DDP has not been fully clarified, it has been associated with failure in the ossification process. Plain radiographs typically show a round lytic lesion in the superolateral aspect of the patella with a peripheral sclerotic margin seen in approximately 0.3-1% of the general population and is often asymptomatic. On MR imaging, DDP is demonstrated as a focal contour abnormality **(Fig. 9a)** [36]. In elite athletes with patellar pain, in whom MR imaging does not disclose the source of pain, MR or Cone Beam CT arthrography may be indicated in order to skip unnecessary arthroscopy **(Fig. 9b)** [37]. Symptomatic DDP is related to articular cartilage disruption by the underlying osseous defect and non-operative treatment is initially recommended with surgery reserved for persisting cases [38]. The presence of BME is suggestive of a symptomatic lesion **(Fig. 9c)**. The main differential diagnoses for DDP are *osteochondritis dissecans* (OCD) and chondroblastoma. OCD is rare, occurs typically in males 15 to 20-year-old, the presence of an osseous fragment favours the diagnosis and the presence of a high signal intensity interface between the fragment and the host bone suggests instability. Giant cell tumour and intraosseous gout are rarely located in the patella [39, 40] **(Fig. 10)**.

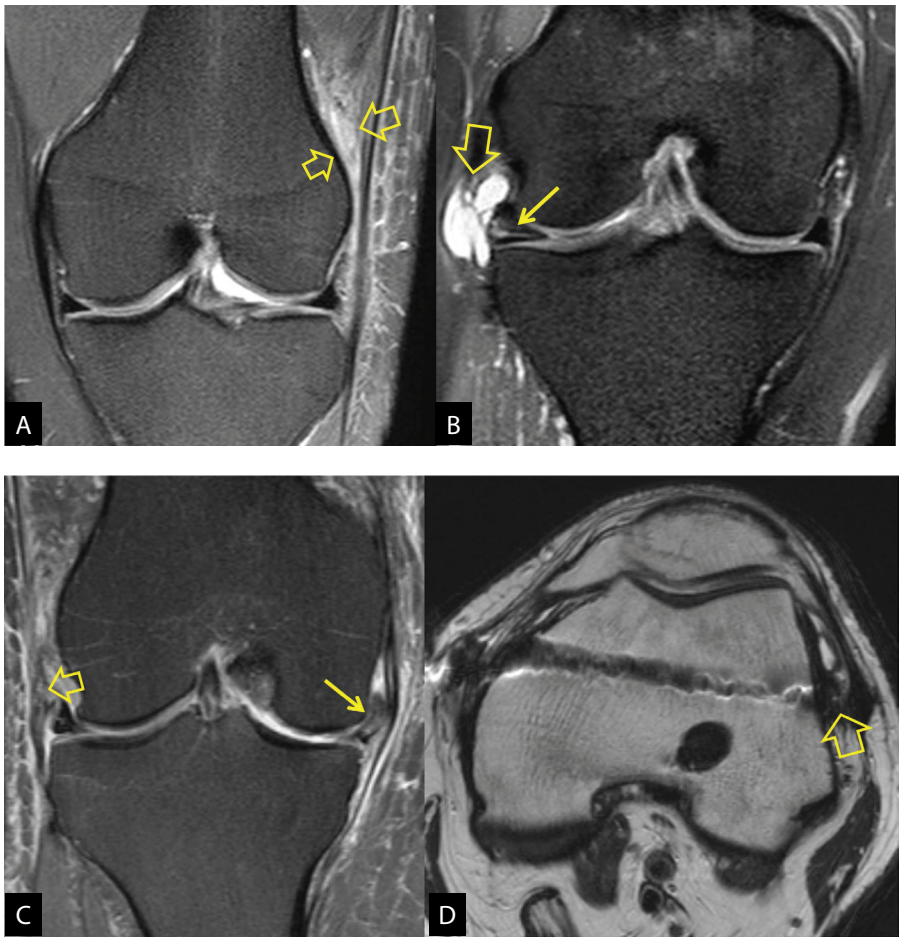

Fig. 14. *Lateral knee joint pain. Coronal fat suppressed PD-w (A-C) and axial T2-w (D) MR images.* ***A.*** *Soft tissue oedema is shown between the lateral femoral epicondyle and the iliotibial band (open arrows) in this 22-year-old avid cyclist and runner with clinically present iliotibial band syndrome.* ***B.*** *A 34-year-ol female, previously elite voleyball player, with lateral knee pain. Horizontal lateral meniscus tear (arrow) and parameniscal cyst (open arrow) are shown.* ***C.*** *A 42-year-old female mountain trekker with a history of rotational injury shows tear of the anterolateral ligament (open arrow). A minimally symptomatic medial meniscal tear from an older injury is also shown (arrow).* ***D.*** *Impingement of the iliotibial band over a projecting screw. Oedema and fibrosis are shown between the lateral femoral condyle and the iliotibial band (open arrow) in this 42-year-old with 1-year anterolateral knee pain following previous ACL reconstruction.*

3.3 Supra/retropatellar space

The supra/retropatellar space consists of the insertion of the QFt onto the upper pole of the patella, the SPFP and PFFP. Altered biomechanics or chronic tensile forces to the QFt, such as in jumping sports, may lead to chronic tendinosis of the tendon that clinically may present as AKP. Acute QFt ruptures occur in sports injuries or in older than 40-year-old patients with previous tendinopathy or other underlying systemic disease, predisposing to tendon degeneration and tear [41]. Typically, QFt tear occurs following eccentric loading with the knee flexed. Injuries in the myotendinous junction are usually seen in athletes. MR imaging findings in tendinopathy are the same as in other tendons, showing abnormal signal intensity in all pulse sequences, particularly on fluid sensitive ones, with or without tendon swelling (**Fig. 11a, c**). Partial or complete tear is shown with focal areas of high signal intensity or discontinuity (**Fig. 11a, b**). Grade I myotendinous strain appears on MR images as interstitial oedema at the myotendinous junction with some extension to adjacent muscle. Grade II injury usually demonstrates a haematoma at the myotendinous junction and in surrounding fascia on MR images. Grade III injury results in muscle retraction and often in haemat-

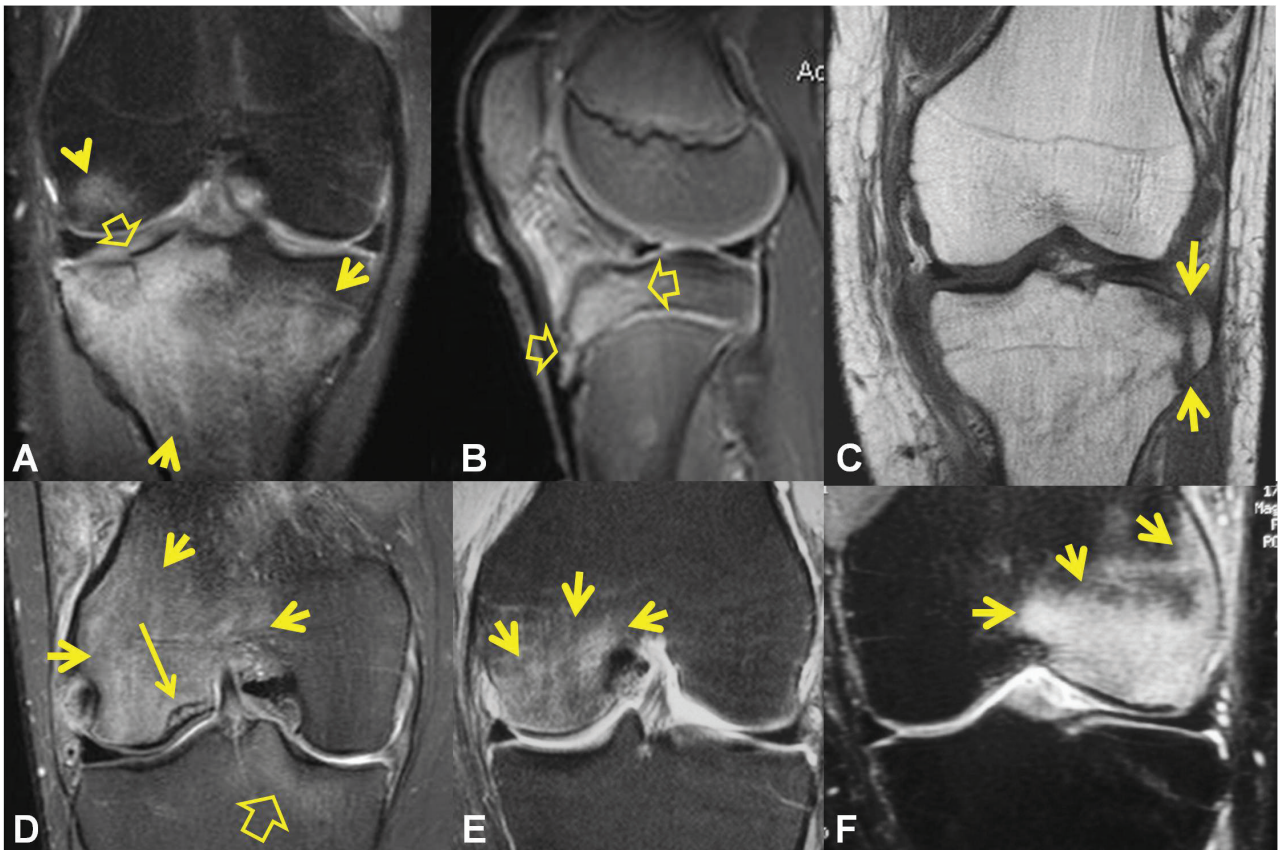

Fig. 15. A. *A 21-year-old male with a history of an overextension injury 3 weeks prior to imaging. The plain radiographs were normal. A. The coronal fat suppressed PD-w TSE MR image shows extensive bone marrow oedema-like pattern (arrows), more prominent in the tibia and an occult fracture of the lateral tibial plateau with cortical disruption and 2-mm depression (open arrow).* ***B.*** *Sagittal fat suppressed PD-w MR image in a 9-year-old football player without injury, presenting with anterolateral knee pain improving at rest, shows bone marrow oedema in keeping with a stress reaction in anterolateral tibial epiphysis and the tibial tubercle (open arrows). Oedema is shown in the Hoffa' s fat pad. The clinical diagnosis suggested erroneously Osgood-Schlatter disease.* ***C.*** *A 24-year-old male with a history of motor vehicle accident 10 days prior to imaging. The coronal T1-w MR image shows a Segond avulsion fracture (arrows).* ***D.*** *Transient bone marrow oedema (transient osteoporosis) in a 52-year-old male patient with a 3-weeks lateral knee joint pain without any history of trauma. The coronal fat suppressed PD-w MR image shows extensive lateral femoral condyle bone marrow oedema (arrows). The low signal intensity linear structures represent trabecular subchondral insufficiency microfractures (thin arrow) without any irregularity in the overlying articular surface. There is also minor degree of marrow oedema in the medial tibial epiphysis (open arrow). Regional migratory osteoporosis in a 35-year-old male with proven Vit. D insufficiency. Coronal fat suppressed PD-w MR image* ***(E)*** *at 3 weeks from onset of medial knee joint pain shows bone marrow oedema (arrows).* ***F.*** *Patient presents with anterolateral knee pain 13 months later. Coronal fat suppressed T2-w MR image shows complete resolution of bone marrow oedema in the medial femoral condyle and new marrow oedema in the lateral femoral condyle (arrows). Spinal DEXA at this stage showed a T score of -3.3.*

omas or oedema. Ultrasonography shows high accuracy and clinical utility in assessing the QT disorders, whereas is able to guide intervention for the treatment of tendinopathy [42, 43].

The *SPFP* has a triangular shape and is the smallest of the fat pads in the anterior knee, measuring 6-7 mm. It is separated posteriorly from the PFFP by the joint recess. Oedema within the SPFP is seen in 4-14% of knee MR imaging examinations and is more prevalent in young male patients [44-46]. Mass effect with convex appearance has been used as a criterion for oedematous swelling of the SPFP [47]. SPFP oedema correlation with AKP however is debatable. Accord-

ing to a report, AKP occurs in about 5% of cases with SPFP oedema and therefore careful matching of imaging findings with clinical symptoms should precede the interpretation of images **(Fig. 11 c, d)** [46]. *PFFP* oedema rarely occurs in the context of impingement of the QFt over the anterior distal femoral bone and has been reported to occur often in asymptomatic swimmers [48]. There are no major reports regarding this disorder which is thought to be underdiagnosed. AKP and fat pad oedema on fluid sensitive MR images may be seen in association with extensor mechanism dysplasia of any kind **(Fig. 11e, f)** [49].

3.4 Infra/retropatellar space

Patellar tendinopathy is the most common disorder of the Pt and is a common cause of AKP (41). It is usually seen in the proximal part of the Pt in young athletes involved in running or jumping, also known as "jumper's knee'. MR imaging is diagnostic showing on fat suppressed images the thickening and abnormal signal of the proximal Pt, primarily affecting the posterior fibers **(Fig. 12a)** [50]. Chronic cases are demonstrated on MR imaging with diffuse Pt thickening showing low signal on all pulse sequences **(Fig. 12b)** whereas diffuse abnormal signal within a thickened Pt represents mucoid degeneration **(Fig. 12c)** [51, 52]. Chronic traction of the Pt at the tibial tubercle results *in Osgood-Schlatter disease* (OSd) which represents an apophysitis in the growing skeleton [53]. The diagnosis is clinical with imaging being reserved for atypical cases with AKP. MR imaging with fat suppressed images shows distal Pt abnormal signal and thickening, fragmentation of the tibial tubercle with BME extending also in the anterior tibia, soft tissue oedema and occasionally retropatellar bursitis. Symptomatic OSd in the adulthood, seen often in jumping sports, is called "unresolved OSd" **(Fig. 12d)**. *Sinding-Larsen-Johansson syndrome* (SLJs) is defined as "apophysitis of the distal pole of the patella" and is the OSd equivalent osteochondrosis at the proximal Pt insertion. SLJs primarily affects adolescents between 10 and 14 years of age, mainly boys, involved in sports. MR imaging findings consist of superior Hoffa's fat pad oedema and inferior patellar pole BME, with or without fragmentation depending upon the duration of symptoms **(Fig. 12e)**. *Partial or full thickness tear* of the Pt represents the end stage of patellar tendinosis and results from the cumulative effect of repetitive trauma and microtearing. Bilateral rupture occurs in the setting of longstanding systemic inflammatory disease, diabetes mellitus and chronic renal failure. MR imaging findings are similar to those of the already described QFt tearing. The largest of the peripatellar fat pads is the *Hoffa's fat pad* (Hfp). This intra-capsular, synovial-lined adipose tissue structure may have a protective function and, although its main role has not been fully clarified, it seems that resection alters the biomechanics of the extensor mechanism [54]. *Superolateral Hoffa fat pad* (SLHFP) oedema is a common and non specific finding in routine MR imaging examinations of the knee both in young athletic and middle aged individuals. The SLHFP oedema may represent the imaging equivalent of the clinical syndrome known as "patellofemoral friction syndrome" demonstrated with AKP and tenderness at the lateral inferior pole of the patella [55]. Associated pain exacerbation with hyperextension suggests patellar maltracking [56-59]. Recent studies suggested that SLHFP oedema may be a marker of structural damage of the patellofemoral joint in patients at risk for development of osteoarthritis [60, 61]. The diffuse inflammation of the Hfp is called "*Hoffa's disease*". The disorder is the result of acute or repetitive trauma. MR imaging is diagnostic by demonstrating high signal intensity on fluid sensitive sequences. Hfp is the location of a wide spectrum of tumours and tumour-like disorders and MR imaging is a powerful tool for accurate diagnosis **(Fig. 13)** [62].

3.5 Lateral non-osseous space

The iliotibial band friction syndrome (ITBFs) is a non-traumatic overuse injury resulting in local irritation and inflammation of the iliotibial band on its distal part. It is a common athletic injury, seen often in runners and cyclists who perform repetitive flexion and extension of the knee. Typically it demonstrates with pain located at the distal iliotibial band, between the lateral epicondyle and the Gerdy's tubercle, exacerbating with activity [63]. Athletes with limb length discrepancy, genu varum, foot overpronation, hip adductor weakness and myofascial restricion are at risk for developing ITBFs [64]. MR imaging findings consist of thickening of the distal iliotibial band and soft tissue oedema over the femoral epicondyle **(Fig. 14)**. According to our experinece (data not published), a single steroid injection without image guidance in the acute/subacute stage of presenting symptoms (less than 4 weeks duration) is beneficial. Rarely, a malposition of a screw in patients who underwent anterior cruciate ligament (ACL) reconstruction may result in ITBFs **(Fig. 14)** [65]. Lateral meniscal tears are com-

mon source of lateral knee joint pain, primarily seen in young adults involved in sports [66-68]. Lateral meniscal tears, particularly the "bucket-handle" type, are rare compared to the medial meniscus equivalent [67]. MR imaging ability to depict lateral meniscus tears is limited, particularly if a discoid morphology coexists [69]. A larger meniscal tear extending into the meniscocapsular junction is more likely to be associated with the occurrence of a parameniscal cyst **(Fig. 14)** [70].

The *ALL* is widely accepted as a distinct component of the anterolateral capsule of the knee joint with consistent origin, rather variant distal insertion and a restraint action to internal rotation of the knee with increasing degrees of flexion [71]. This may explain the persistent anterolateral rotational instability in 10-30% of patients who underwent ACL reconstruction [72]. MR imaging in the coronal plane is the best means of ALL depiction [16, 73, 74]. Studies reported that MRI shows high detection rates of ALL, both in the non injured and injured knee, particularly in combination with ACL tears [75, 76]. Other studies showed that MRI is not a reliable tool to diagnose injury in the setting of concurrent ACL rupture [77-79]. According to recent reported studies, clinical correlation remains essential and thus decision to reconstruct the ALL should not be based on MR imaging alone [79].

3.6 Lateral osseous space

Trauma: MR imaging in *bone bruises* shows a diffuse or localised decreased signal intensity on T1-w and increased signal intensity on fluid sensitive sequences. This appearance is thought to represent areas of haemorrhage, oedema or infarction secondary to trabecular microfractures that may all contribute to marrow signal alterations. The distribution of bone contusion-related BME on MR imaging represents a footprint of the mechanism of injury, and could predict and confirm the presence of capsule ligamentous injuries [80]. Bone bruise located in the lateral femoral condyle has been already discussed as suggesting previous recent lateral patellar dislocation **(Fig. 8)**. The *pivot shift* injury results in BME located at the posterior lateral tibial epiphysis and at the mid-portion of the lateral femoral condyle. The *dashboard* injury results in BME located at the anterolateral tibia, whereas a *hyperextension* injury in BME located at a "kissing" pattern in the anterior femoral condyle and anterior tibial epiphysis. The *clip*, which is a contact injury, results in BME located at the lateral femoral condyle secondary to the direct blow. MR imaging shows lateral tibial plateau fractures and stress reactions **(Fig. 15 a, b)** or Segond fractures, also seen on radiographs and CT **(Fig. 15c)** [81, 82].

Tumours: MR imaging has a complementary role to radiographs and CT in the holistic diagnostic approach of knee joint neoplasias [83].

BME in the knee is a common non specific finding and has already been discussed in the context of acute or repetitive trauma **(Fig. 5, 8, 15a, b)** [84]. Osteoarthritis is often associated with subchondral bone marrow lesions, including BME [85]. Extensive BME without previous trauma has been a matter of debate for many years as misleading terminology including "spontaneous osteonecrosis", "early osteonecrosis", and "chronic regional pain syndrome", has been applied. Currently, the presence of non-traumatic BME is called *transient osteoporosis* or even more accurately aBMEs with a single location or a "migratory" pattern. Typically, aBMEs is seen in middle-aged men or elderly women. On fluid sensitive MR images it appears as an ill-defined high signal intensity lesion in the bone marrow, extending to the articular surface, with or without demonstration of a thin subarticular low signal intensity lesion, which is thought to represent microtrabecular insuffiency fracture **(Fig. 15d)** [30]. Articular collapse may complicate this entity, related to the low bone mineral density as shown with spinal DEXA, increased duration of symptoms before diagnosis and weight bearing protection, previous osteoarthritis, female sex and increased age [30]. Migration of the BME within the joint **(Fig. 6, 15e, f)**, to the contralateral joint or to the ipsilateral hip or foot may occur within a period of few months, is seen almost exclusively in middle aged men and is almost always related to reduced bone mineral density on spine DEXA [86].

4. Conclusion

ALk represents a complex anatomic area including osseous, fatty, tendinous and ligamentous structures. This area is vulnerable to injuries and is the location of a broad group of disorders, afflicting the soft tissues and the osseous structures. Pathology is highly depended upon the age and sex of the patients. MR imaging is a powerful tool for accurate diagnosis. In certain disorders, correlation with clinical history and physical examination findings is of paramount importance in order to arrive to a correct diagnosis. R

Conflict of interest

The authors declared no conflicts of interest.

References

1. James EW, LaPrade CM, LaPrade RF. Anatomy and biomechanics of the lateral side of the knee and surgical implications. *Sports Med Arthrosc* 2015; 23(1): 2-9.
2. Guenther D, Griffith C, Lesniak B, et al. Anterolateral rotator instability of the knee. *Knee Surg Sports Traumatol Arthrosc* 2015; 23(10): 2909-2917.
3. Graham GP, Fairclough JA. Early osteoarthritis in young sportsmen with severe anterolateral instability of the knee. *Injury* 1988; 19(4): 247-248.
4. Ferrer GA, Guentther D, Pauyo T, et al. Structural properties of the anterolateral complex and their clinical implications. *Clin Sports Med* 2018; 37(1): 41-47.
5. Kittl C, Inderhaug E, Williams A, et al. Biomechanics of the anterolateral structures of the knee. *Clin Sports Med* 2018; 37(1): 21-31.
6. Panni AS, Cerciello S, Maffulli N, et al. Patellar shape can be a predisposing factor in patellar instability. *Knee Surg Sports Traumatol Arthrosc* 2011; 19: 663-670.
7. Loudon JK. Biomechanics and pathomechanics of the patellofemoral joint. *Int J Sports Phys Ther* 2016; 11(6): 820-830.
8. Starok M, Lenchik L, Trudell D, et al. Normal patellar retinaculum: MR and sonographic imaging with cadaveric correlation. *AJR Am J Roentgenol* 1997; 168(6): 1493-1499.
9. Shah KN, DeFroda SF, Ware JK, et al. Lateral patellofemoral ligament-an anatomic study. *Orthop J Sports Med* 2017; 5(12): 2325967117741439.
10. Hamill J, Miller R, Noehren B, et al. A prospective study of iliotibial band strain in runners. *Clin Biomech* 2008; 23(8): 1018-1025.
11. Seebacher JR, Inglis AE, Marshall JL, et al. The structure of the posterolateral aspect of the knee. *J Bone Joint Surg Am* 1982; 64(4): 536-541.
12. Dodds AL, Halewood C, Gupte CM, et al. The anterolateral ligament: Anatomy, length changes and association with the Segond fracture. *Bone Joint J* 2014; 96-B(3): 325-331.
13. Claes S, Vereecke E, Maes M, et al. Anatomy of the anterolateral ligament of the knee. *J Anat* 2013; 223(4): 321-328.
14. Caterine S, Litchfeld R, Johnson M, et al. A cadaveric study of the anterolateral ligament: Re-introducing the lateral capsular ligament. *Knee Surg Sports Traumatol Arthrosc* 2015; 23(11): 3186-3195.
15. Daggett M, Ockuly AC, Cullen M, et al. Femoral origin of the anterolateral ligament: an anatomic analysis. *Arthroscopy* 2016; 32(5): 835-841.
16. Klontzas ME, Maris TG, Zibis AH, et al. Normal magnetic resonance imaging anatomy of the anterolateral knee ligament with a T2/T1-weighted 3-dimensional sequence: a feasibility study. *Can Assoc Radiol J* 2016; 67(1): 52-59.
17. Spencer L, Burkhart TA, Tran MN, et al. Biomechanical analysis of simulated clinical testing and reconstruction of the anterolateral ligament of the knee. *Am J Sports Med* 2015; 43(9): 2189-2197.
18. Parsons EM, Gee AO, Spiekerman C, et al. The biomechanical function of the anterolateral ligament of the knee. *Am J Sports Med* 2015; 43(3): 669-674.
19. Jacobson JA, Lenchik L, Ruboy MK, et al. MR imaging of the infrapatellar fat pad of Hoffa. *Radiographics* 1997; 17(3): 675-691.
20. Bellon EM, Sacco DC, Steiger DA, et al. MRI in "housemaid's knee" (prepatellar bursitis). *Magn Reson Imaging* 1987; 5(3): 175-177.
21. Bonilla-Yoon I, Masih D, Paterl DB, et al. The Morel-Lavallée lesion: Pathophysiology, clinical presentation, imaging features, and treatment options. *Emerg Radiol* 2014; 21(1): 35-43.
22. Mellado JM, Bencardino JT. Morel-Lavallée lesion: Review with emphasis on MR imaging. *Magn Reson Imaging Clin N Am* 2005; 13(4): 775-782.
23. Borrero CG, Maxwell N, Kavanagh E. MRI findigns of prepatellar Morel- Lavallée effusions. *Skeletal Radiol* 2012; 37: 451-455.
24. Vassalou EE, Zibis AH, Raoulis VA, et al. Morel-Lavallée lesions of the knee: MR Imaging findings compared with a cadaveric study. *AJR Am J Roentgenol 2018 (in press)*. doi.org/10.2214/AJR.17.18614.
25. Diviti S, Gupta N, Hooda K, et al. Morel-Lavallée lesions-review of pathophysiology, clinical findings, imaging findigns and management. *J Clin Diagn Res* 2017; 11(4): TE1-TE4.
26. Vanhoenacker F, De Vos N, Van Dyck P. Common mistakes and pitfalls in magnetic resonance imaging of the knee. *J Belg Soc Radiol* 2016; 100(1): 1-17.

27. Weaver JK. Bipartite patellae as a cause of disability in the athlete. *Am J Sports Med* 1977; 5(4): 137-143.
28. Iwamoto J, Takeda T. Stress fractures in athletes: Review of 196 cases. *J Orthop Sci* 2003; 8(3): 273-278.
29. Behrens SB, Deren ME, Matson A, et al. Stress fractures of the pelvis and legs in athletes: A review. *Sports Health* 2013; 5(2): 165-174.
30. Karantanas AH, Drakonaki E, Karachalios T, et al. Acute non-traumatic marrow edema syndrome in the knee: MRI findings at presentation, correlation with spinal DEXA and outcome. *Eur J Radiol* 2008; 67(1): 22-33.
31. Hunt DM, Somashekar N. A review of sleeve fractures of the patella in children. *Knee* 2005; 12(1): 3-7.
32. Earhart C, Patel DB, White EA, et al. Transient lateral patellar dislocation: Review of imaging findings, patellofemoral anatomy, and treatment options. *Emerg Radiol* 2013; 20(1): 11-23.
33. Köhlitz T, Scheffler S, Jung T, et al. Prevalence and patterns of anatomical risk factors in patients after patellar dislocation: A case control study using MRI. *Eur Radiol* 2013; 23(4): 1067-1074.
34. Tsavalas N, Katonis P, Karantanas AH. Knee joint anterior malalignment and patellofemoral osteoarthritis: An MRI study. *Eur Radiol* 2012; 22(2): 418-428.
35. Karachalios T, Zibis A, Papanagiotou P, et al. MR imaging findings in early osteoarthritis of the knee. *Eur J Radiol* 2004; 50(3): 225-230.
36. Ho VB, Kransdorf MJ, Jelinek JS, et al. Dorsal defect of the patella: MR features. *J Comput Assist Tomogr* 1991; 15(3): 474-476.
37. Posadzy M, Desimpel J, Vanhoenacker F. Cone beam CT of the musculoskeletal system: Clinical applications. *Insights Imaging* 2018; 9(1): 35-45.
38. Kwee TC, Sonneveld H, Nix M. Successful conservative management of symptomatic bilateral dorsal patellar defects presenting with cartilage involvement and bone marrow edema: MRI findings. *Skeletal Radiol* 2016; 45(5): 723-727.
39. Singh J, James SL, Kroon HM, et al. Tumour and tumour-like lesions of the patella-a multicentre experience. *Eur Radiol* 2009(3); 19: 701-712.
40. Casadei R, Kreshak J, Rinaldi R, et al. Imaging tumors of the patella. *Eur J Radiol* 2013; 82(12): 2140-2148.
41. Yablon CM, Pai D, Dong Q, et al. Magnetic resonance imaging of the extensor mechanism. *Magn Reson Imaging Clin N Am* 2014; 22(4): 601-620.
42. McMahon CJ, Ramappa A, Lee K. The extensor mechanism: Imaging and intervention. *Semin Musculoskelet Radiol* 2017; 21(2): 89-101.
43. Ostlere S. The extensor mechanism of the knee. *Radiol Clin N Am* 2013; 51(3): 393-411.
44. Roth C, Jacobson J, Jamadar D, et al. Quadriceps fat pad signal intensity and enlargement on MRI: Prevalence and associated findings. *AJR Am J Roentgenol* 2004; 182(6): 1383-1387.
45. Shabshin N, Schweitzer ME, Morrison WB. Quadriceps fat pad edema: Significance on magnetic resonance images of the knee. *Skeletal Radiol* 2006; 35(5): 269-274.
46. Tsavalas N, Karantanas AH. Suprapatellar fat-pad mass effect: MRI findings and correlation with anterior knee pain. *AJR Am J Roentgenol* 2013; 200(3): W291-296.
47. Samin M, Smitaman E, Lawrence D, et al. MRI of anterior knee pain. *Skeletal Radiol* 2014; 43(7): 875-893.
48. Soder RB, Mizerkowski MD, Petkowicz R, et al. MRI of the knee in asymptomatic adolescent swimmers: A controlled study. *Br J Sports Med* 2012; 46(4): 268-272.
49. Grando H, Chang EY, Chen KC, et al. MR imaging of extrasynovial inflammation and impingement about the knee. *Magn Reson Imaging Clin N Am* 2014; 22(4): 725-741.
50. Johnson DP, Wakeley CJ, Watt I. Magnetic resonance imaging of patellar tendonitis. *J Bone Joint Surg Br* 1996; 78(3): 452-457.
51. O'Keeffe SA, Hogan BA, Eustace SJ, et al. Overuse injuries of the knee. *Magn Reson Imaging Clin N Am* 2009; 17(4):725-739.
52. Peace KA, Lee JC, Healy J. Imaging the infrapatellar tendon in the elite athlete. *Clin Radiol* 2006; 61(7): 570-578.
53. Hirano A, Fukubayashi T, Ishii T, et al. Magnetic resonance imaging of Osgood-Schlatter disease: The course of the disease. *Skeletal Radiol* 2002; 31(6): 334-342.
54. Bohnsack M, Wilharm A, Hurschler C, et al. Biomechanical and kinematic influences of a total infrapatellar fat pad resection on the knee. *Am J Sports Med* 2004; 32(8): 1873-1880.
55. Chung CB, Skaf A, Roger B, et al. Patellar tendon-lateral femoral condyle friction syndrome: MR imaging in 42 patients. *Skeletal Radiol* 2001; 30(12): 694-697.
56. Jarraya M, Diaz LE, Roemer FW, et al. MRI findings

consistent with peripatellar fat pad impingement: how much related to patellofemoral maltracking? *Magn Reson Med Sci* 2017; Oct 10. doi: 10.2463/mrms.rev. 2017-0063. [Epub ahead of print].
57. Matcuk GR Jr, Cen SY, Keyfes V, et al. Superolateral hoffa fat-pad edema and patellofemoral maltracking: predictive modeling. *AJR Am J Roentgenol* 2014; 203(2): W207-212.
58. Campagna R, Pessis E, Biau DJ, et al. Is superolateral Hoffa fat pad edema a consequence of impingement between lateral femoral condyle and patellar ligament? *Radiology* 2012; 263(2): 469-474.
59. De Smet AA, Davis KW, Dahab KS, et al. Is there an association between superolateral Hoffa fat pad edema on MRI and clinical evidence of fat pad impingement? *AJR Am J Roentgenol* 2012; 199(5): 1099-1104.
60. Jarraya M, Guermazi A, Felson DT, et al. Is superolateral Hoffa's fat pad hyperintensity a marker of local patellofemoral joint disease? - The MOST study. Osteoarthritis Cartilage 2017; 25(9): 1459-1467.
61. Widjajahakim R, Roux M, Jarraya M, et al. Relationship of trochlear morphology and patellofemoral joint alignment to superolateral hoffa fat pad edema on MR Images in individuals with or at risk for osteoarthritis of the knee: The MOST study. *Radiology* 2017; 284(3): 806-814.
62. Jacobson JA, Lenchik L, Ruhoy MK, et al. MR imaging of the infrapatellar fat pad of Hoffa. *Radiographics* 1997; 17(3): 675-691.
63. Flato R, Passanante GJ, Skalski MR, et al. The iliotibial tract: Imaging, anatomy, injuries, and other pathology. *Skeletal Radiol* 2017; 46(5): 605-622.
64. Vasilevska V, Szeimies U, Stäbler A. Magnetic resonance imaging signs of iliotibial band friction in patients with isolated medial compartment osteoarthritis of the knee. *Skeletal Radiol* 2009; 38(9): 871-875.
65. Cruz-López F, Mallen-Trejo A, Pascual-Vidriales C, et al. Iliotibial band friction syndrome due to bioabsorbable pins in ACL reconstruction. *Acta Ortop Mex* 2016; 30(6): 307-310.
66. Fox MG. MR Imaging of the meniscus: Review, current trends, and clinical implications. *Magn Reson Imaging Clin N Am* 2007; 15(1): 103-123.
67. Nguyen JC, De Smet AA, Graf BK, et al. MR imaging-based diagnosis and classification of meniscal tears. *Radiographics* 2014; 34(4): 981-999.
68. Wadhwac V, Omar H, Coyner K, et al. ISAKOS classification of meniscal tears-illustration on 2D and 3D isotropic spin echo MR imaging. *Eur J Radiol* 2016; 85(1): 15-24.
69. Ryu KN, Kim IS, Kim EJ, et al. MR imaging of discoid lateral menisci. *AJR Am J Roentgenol* 1998; 171(4): 963-967.
70. Wu CC, Hsu YC, Chiu YC, et al. Parameniscal cyst formation in the knee is associated with meniscal tear size: An MRI study. *The Knee* 2013; 20(6): 556-561.
71. Van Dyck P, De SMet E, Lambrecht V, et al. The anterolateral ligament of the knee: What the radiologist needs to know. *Semin Musculoskelet Radiol* 2016; 20(1): 26-32.
72. Murawski CD, van Eck CF, Irrgang JJ, et al. Operative treatment of primary anterior cruciate ligament rupture in adults. *J Bone Joint Surg Am* 2014; 96(8): 685-694.
73. Helito CP, Helito PV, Costa HP, et al. MRI evaluation of the anterolateral ligament of the knee: Assessment in routine 1.5-T scans. *Skeletal Radiol* 2014; 43(10): 1421-1427.
74. Taneja AK, Miranda FC, Braga CA, et al. MRI features of the anterolateral ligament of the knee. *Skeletal Radiol* 2015; 44(3): 403-410.
75. Claes S, Bartholomeeusen S, Bellemans J. High prevalence of anterolateral ligament abnormalities in magnetic resonance images of anterior cruciate ligament-injured knees. *Acta Orthop Belg* 2014; 80(1): 45-49.
76. Faruch Bilfeld M, Cavaignac E, Wytrykowski K, et al. Anterolateral ligament injuries in knees with an anterior cruciate ligament tear: Contribution of ultrasonography and MRI. *Eur Radiol* 2018; 28(1): 58-65.
77. Hartigan DE, Carroll KW, Kosarek FJ, et al. Visibility of anterolateral ligament tears in anterior cruciate ligament-deficient knees with standard 1.5-Tesla magnetic resonance imaging. *Arthroscopy* 2016; 32(10): 2061-2065.
78. Kosy JD, Schranz PJ, Patel A, et al. The magnetic resonance imaging appearance of the anterolateral ligament of the knee in association with anterior cruciate rupture. *Skeletal Radiol* 2017; 46(9): 1193-1200.
79. Devitt BM, O'Sullivan R, Feller JA, et al. MRI is not reliable in diagnosing of concomitant anterolateral ligament and anterior cruciate ligament injuries of the knee. *Knee Surg Sports Traumatol Arthrosc* 2017; 25(4): 1345-1351.

80. Sanders TG, Medynski MA, Feller JF, et al. Bone contusion patterns of the knee at MR imaging: Footprint of the mechanism of injury. *Radiographics* 2000; 20: S135-S151.
81. Matcuk GR Jr, Mahanty SR, Skalski MR, et al. Stress fractures: Pathophysiology, clinical presentation, imaging features, and treatment options. *Emerg Radiol* 2016; 23(4): 365-375.
82. Claes S, Luyckx T, Vereecke E, et al. The Segond fracture: a bony injury of the anterolateral ligament of the knee. *Arthroscopy* 2014; 30(11): 1475-1482.
83. Freeman AK, Sumathi VP, Jeys L. Primary malignant tumours of the bone. *Surgery* 2018; 36(1): 27-34.
84. Toms AP, Fowkes LA. Bone marrow oedema of the knee. *The knee* 2010; 17(1): 1-6.
85. Crema MD, Roemer FW, Zhu Y, et al. Subchondral cystlike lesions develop longitudinally in areas of bone marrow edema-like lesions in patients with or at risk for knee osteoarthritis: Detection with MR imaging-the MOST study. *Radiology* 2010; 256(3): 855-862.
86. Karantanas AH, Nikolakopoulos I, Korompilias AV, et al. Regional migratory osteoporosis in the knee: MRI findings in 22 patients and review of the literature. *Eur J Radiol* 2008; 67(1): 34-41.

READY - MADE CITATION

Smarlamaki RM, Terezaki FI, Savva ED, Karantanas A. MR Imaging of anterolateral knee pain. *Hell J Radiol* 2018; 3(1): 45-60.